Available online at www.sciencedirect.com

ScienceDirect

journal homepage: www.elsevier.com/locate/he

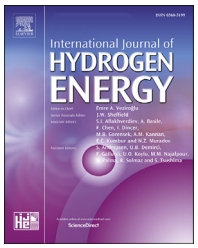

Dynamic simulation of different transport options of renewable hydrogen to a refinery in a coupled energy system approach

Lisa Andresen[*], *Carsten Bode*, *Gerhard Schmitz*

Hamburg University of Technology, Institute of Engineering Thermodynamics, Denickestrasse 17, 21073 Hamburg, Germany

ARTICLE INFO

Article history:
Received 10 January 2018
Received in revised form
13 August 2018
Accepted 16 August 2018
Available online 21 September 2018

Keywords:
Power-to-gas
Hydrogen substitution in a refinery
Transportation infrastructure
Production cost
CO_2 emission
Dynamic simulation

ABSTRACT

Three alternative transport options for hydrogen generated from excess renewable power to a refinery of different scales are compared to the reference case by means of hydrogen production cost, overall efficiency, and CO_2 emissions. The hydrogen is transported by a) the natural gas grid and reclaimed by the existing steam reformer, b) an own pipeline and c) hydrogen trailers. The analysis is applied to the city of Hamburg, Germany, for two scenarios of installed renewable energy capacities. The annual course of excess renewable power is modeled in a coupled system approach and the replaceable hydrogen mass flow rate is determined using measurement data from an existing refinery. Dynamic simulations are performed using an open-source Modelica® library. It is found that in all three alternative hydrogen supply chains CO_2 emissions can be reduced and costs are increased compared to the reference case. Transporting hydrogen via the natural gas grid is the least efficient but achieves the highest emission reduction and is the most economical alternative for small to medium amounts of hydrogen. Using a hydrogen pipeline is the most efficient option and slightly cheaper for large amounts than employing the natural gas grid. Transporting hydrogen by trailers is not economical for single consumers and realizes the lowest CO_2 reductions.

Introduction

The 2015 United Nations Climate Change Conference emphasized again the aim to reduce climate change. Within the negotiated Paris Agreement, in which the participating countries want to achieve greenhouse gas (GHG) neutrality in the second half of this century [1], Germany aims to reduce GHG emissions by at least 80–95% until 2050 compared to 1990 [2]. CO_2, with a share of about 88%, is the main causer of GHG emissions [3]. Therein, energy conversion processes are responsible for about 96% and industrial processes for about 5.6% - the difference is due to natural capturing. The main CO_2 reduction measure is to increase renewable power converters. However, the electricity sector is only responsible for about 42% of the energy-related CO_2 emissions. Hence, further reductions in the heating, mobility, and industry sectors are necessary. The latter has a significant hydrogen demand of

* *Corresponding author.*
E-mail addresses: andresen@tuhh.de (L. Andresen), c.bode@tuhh.de (C. Bode), schmitz@tuhh.de (G. Schmitz).
https://doi.org/10.1016/j.ijhydene.2018.08.111

over 60 million tons worldwide of which 95% are supplied by fossil fuels [4]. Thus, there is a great potential which can already be used today.

Often, renewable hydrogen is mentioned as one key technology for sector coupling, as it is generated from renewable electricity by water electrolysis and can then be used in different ways: for electricity generation later in times of lack of renewable supply, for heat generation, as fuel in the transportation sector or as a product in industry [5,6]. The conversion from renewable electricity into chemical energy of gas is often referred to as *Power-to-Gas* (PtG) [5–7]. Especially proton exchange membrane (PEM) electrolyzers have fast response times and can follow renewable generation or excess power curves almost instantaneously. One option to provide renewable hydrogen to all consumers, is the injection into the natural gas grid under certain limitations, e.g. maximum hydrogen concentration [8]. To avoid this limit, hydrogen can be transformed to methane using CO_2 [5–7,9,10].

To decarbonize mobility sector, this hydrogen can be used to produce synthetic fuels (Power-to-Liquid) which can replace fossil fuels. The most promising processes are the Fischer-Tropsch synthesis and the methanol synthesis [11]. Different studies show that these processes are not yet economically feasible but with sufficiently high CO_2 prices, cost parity should be reached not later than 2050 [11–13]. A less costly interim solution is decarbonizing fossil fuels by introducing renewable hydrogen in the refining process.

In refineries, 25.5% of the worldwide produced hydrogen is used and it is mostly produced via steam methane reforming of hydrocarbons [14] which generates CO_2 emissions directly at the refinery. To avoid these emissions and thus decarbonize the refinery products, one option is to replace the internally generated hydrogen by the externally generated power-to-gas product. A comparison of these two hydrogen streams by Al-Subaie et al. [15] shows that steam methane reforming is cheaper for low natural gas prices and low CO_2 prices. With rising CO_2 prices, the operation of the electrolyzer becomes economically efficient. In general, PtG operated by renewable excess power is not seen as necessary until at least 2030 due to the low availability of surplus energy [16].

However, excess power exports from one region to another can be reduced by using it to produce hydrogen in an electrolyzer and injecting it into the natural gas grid [17–19]. When assuming natural gas prices for the admixed hydrogen, this is not economically efficient, though. With high capacity factors and selling the hydrogen to the industry or mobility sector, significant revenues can be generated [5,14].

Other challenges are to match the hydrogen demand with the variable supply of renewable energy sources and to deliver the hydrogen in a cost-efficient way. Different studies have already been conducted about this topic. In the H2A study [20] a spreadsheet tool was developed to compare different transportation options except for the option in which hydrogen is injected into the natural gas grid. Yang and Ogden [21] and Cheng and Graham [22] compared compressed gas and liquid hydrogen trailers and pipelines and they obtained, that compressed gas trailers are the best option for small amounts and short distances, liquid hydrogen trailers are most economic for medium amounts and long distances and pipelines should be preferred for large amounts.

Garmsiri et al. [23] have conducted a study about injection of hydrogen into the natural gas grid and they showed that different sizes of electrolyzers (25–200 MW_{el}) lead to payback periods of 12.8–14.4 years for an Ontario wind farm. Andresen and Schmitz [24] studied hydrogen production from excess renewable power generation and the injection into the natural gas grid in Hamburg. They found a maximum reduction potential of CO_2 emissions of 11.5%. The only comparison of hydrogen injection with other transportation options found was made by Schiebahn et al. [5]. The results show that the transportation of pure hydrogen and the utilization in the transport sector is more economic than injecting hydrogen into the natural gas grid and using it for heating etc.

All studies use simplified stationary models whereas in this work dynamic effects are considered. To the best of the authors' knowledge, no comparison of hydrogen transportation by trailers, a hydrogen pipeline and the natural gas grid, in which pure hydrogen is consumed by the end user, was done so far.

The assessment carried out in the following gives insight into replacement potentials of hydrogen, technical constraints, as well as costs and CO_2 reduction potentials of different transportation pathways using dynamic simulations in a coupled energy system approach. In the considered reference case, hydrogen is produced in a refinery via steam methane reforming. The refinery process and its location are modeled based on an existing refinery in Hamburg. For the scenario variations, measurement data of the refinery is analyzed and it is obtained how much of the internally produced hydrogen can be replaced by externally supplied renewable hydrogen. To increase the informative value, the refinery size and therefore the replaceable hydrogen amount is twice scaled up and twice scaled down which results in five cases. Furthermore, two scenarios of installed renewable energies (RE), RE+ and RE++, are evaluated to consider the effect of an increasing renewable power input and thus availability of excess power. The surplus power is obtained by modeling the coupled electricity and district heating systems of Hamburg. A model of a power-to-gas plant, consisting of an electrolyzer and optional storage and compressor units, is developed and its size economically optimized for the different considered scenarios. Three hydrogen transportation pathways are modeled and evaluated to determine the best option for each scenario in terms of efficiency, CO_2 emissions, and costs: hydrogen is transported by a) the natural gas grid, b) an own pipeline, and c) trailers.

Background

Energy system of Hamburg

Hamburg is the second largest city in Germany and the biggest energy consumer in Northern Germany. It is surrounded by countryside and the North and Baltic Seas, where onshore and offshore wind turbines are excessively installed. Only a small amount of the produced electricity can be used locally. On the other hand, Hamburg is not able to supply itself with sufficient energy but depends to about three quarters on electricity imports [25]. As can be seen in Fig. 1, Hamburg is an example

for an energy system that depends on various line-based energy carriers, i.e. electricity, district heating and gas networks. The displayed high-pressure gas grid and the coupling of electricity and district heating networks via cogeneration plants are modeled in this study. The figure also reveals the location of the investigated crude oil refinery and the assumed location of the power-to-gas plant (PtGP). Close to the place shown here, a 1 MW_{el} PEM electrolyzer pilot plant was built in 2013 in order to investigate the admixture of hydrogen to the high pressure natural gas grid [26]. In the Northern German area, quite a few salt domes exist that can be exploited for underground gas storage. For this study the salt dome directly underneath the PtGP is considered for hydrogen storage.

Hydrogen transport systems

The evaluated hydrogen transport pathways to the refinery are depicted in Fig. 2. One indirect and two direct supply chains are compared to the reference case, in which hydrogen is produced by steam methane reforming of internally generated refinery gases and butane. In contrary to butane, the refinery gases must be processed completely in the steam methane reformer (SMR) because they cannot be sold. Moreover, a certain amount of butane is always fed to the SMR to secure the supply in case of a disturbance in the refinery gas feed. The resulting replaceable amount of butane is sold and replaced by renewably generated hydrogen which is transported by the three analyzed cases. In the indirect pathway (H2NG) the hydrogen is fed into the high pressure natural gas grid. At the SMR a connection to the natural gas grid already exists and whether butane or natural is used, usually depends on their prices. For H2NG the substitutable part of the butane is replaced completely by the natural gas mixture. Although the injected hydrogen does not physically reach the refinery, it is completely accredited to it. Thus, by energetically interchanging part of the natural gas by the admixed hydrogen, CO_2 emissions are reduced. In the two direct pathways, H2Pipe and H2Trailer, the renewable hydrogen is not processed through the SMR but used directly for the consumers at the refinery. The steam reformer is operated in parallel to produce the non-replaceable part of hydrogen with the refinery gases and the non-substitutable part of the butane. For H2Pipe a hydrogen pipeline is assumed to be built next to the southern high pressure natural gas pipeline depicted in Fig. 1. It is operated lightly above the consumer pressure. For H2Trailer at least two trailers go from the PtG site to the refinery and back. The distance and driving times are obtained from street maps. An additional buffer storage, which is installed above ground at the refinery site, economically optimizes the number of trailers.

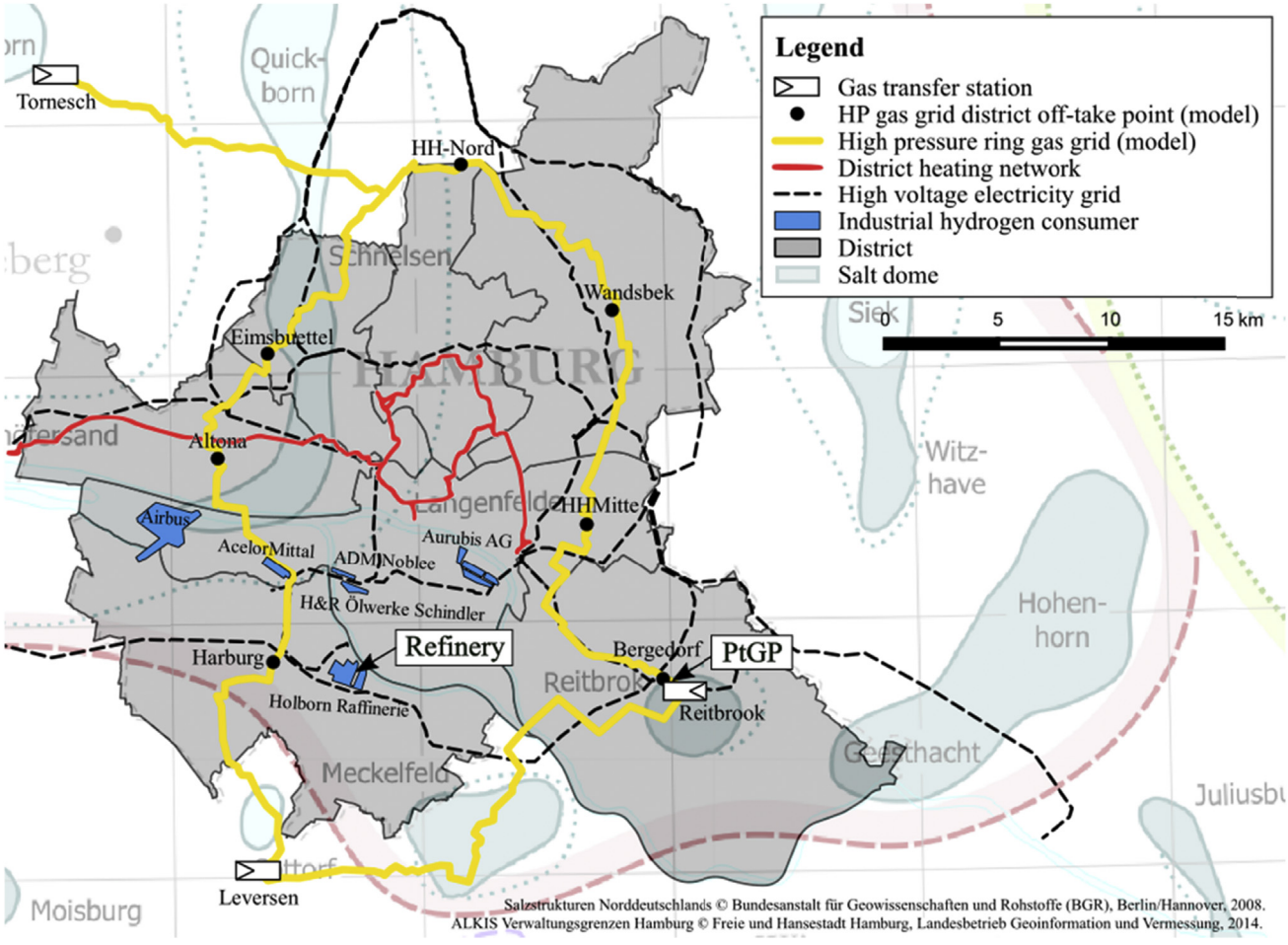

Fig. 1 – City of Hamburg with rough grid layouts and geographic setup. Own representation with data from Refs. [27–29], created with [30].

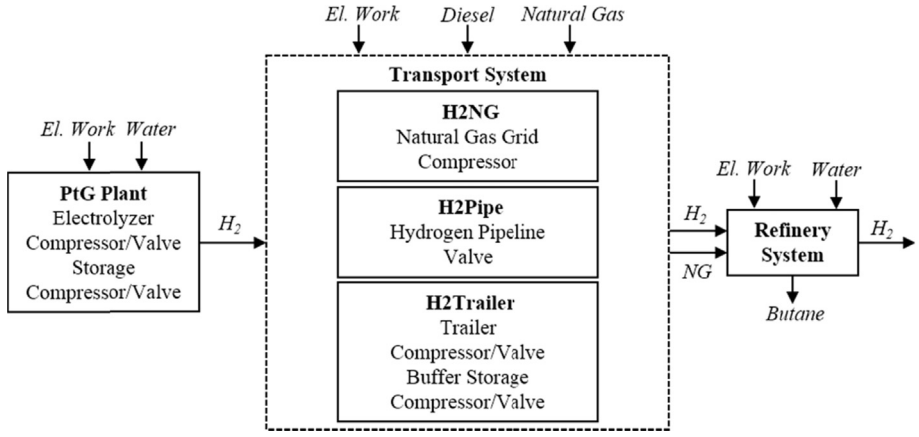

Fig. 2 – Scheme of the investigated system with the three transportation pathways and considered energy flows.

The power-to-gas plant

A PtGP consists of a water electrolyzer, optional compressors, an optional storage unit, and measurement and control devices [31]. Different electrolyzer technologies are state of the art. Even though the alkaline electrolysis technology is the most advanced, the proton exchange membrane (PEM) technology has become the most popular choice for the coupling with renewable energy sources because PEM electrolyzers have short response times and can follow renewable generation profiles easily. For compression of hydrogen, nowadays usually ionic compressors are used. In piston compressors, the lubricant would impurify the hydrogen and hydrogen loss would occur because of the small molecule size. Also, the work needed for compression is bigger compared to an ionic compressor. The choice of the storage technology depends mainly on the volumetric capacity. Big volumes are easily stored in salt caverns, medium volumes in underground pipe storages and small volumes in storage tanks in spherical or cylindrical shape above ground. Methanation of hydrogen is not considered because the higher costs for the methanation unit would exceed the savings in storage in this case.

The crude oil refinery

In a refinery, pure hydrogen is used for desulphurization, hydrogenation, hydrocracking and hydroconversion of distillates and heavy residues of crude oil. Usually hydrogen is produced on-site by steam reforming of refinery gases and butane or natural gas [32]. The refinery gases have a high hydrogen share and are byproducts of different processes, e.g. catalytic reforming and flushing of hydrotreaters.

The Holborn Europa Raffinerie uses a side-fired steam methane reformer (SMR) to produce hydrogen from refinery gases and butane [33]. The system is shown in Fig. 3. First, the refinery gas and butane are mixed and desulphurized because hydrogen sulfide is a strong catalyst poison. Then, the feed is mixed with steam and pre-reformed to break the heavy hydrocarbons into smaller components. In the SMR, methane and steam are transformed into hydrogen and carbon monoxide and carbon dioxide. Thereafter, the hydrogen yield is further increased by the reaction of carbon monoxide into carbon dioxide in the water gas shift (WGS) reactor. In the last two steps, water is extracted and the hydrogen is purified using pressure swing adsorption (PSA). The off-gas is led to the burners which deliver the heat for the endothermic reactions in the SMR. In between these components, there are several heat exchangers to heat up or cool down the respective mass flows.

Modeling and simulation

Modeling

The models are taken from a free modeling library, the *TransiEnt Library*, which is being developed for the dynamic simulation of coupled energy supply systems with high shares of renewable energies [34–36]. The non-proprietary modeling language Modelica® [37] and the simulation environment Dymola™ [38] are used to mathematically describe the stakeholders of energy supply systems. The considered physical effects of the main components of the here investigated systems are explained briefly in the following and simulation input parameters are displayed in Table 1.

Refinery System: All component models except for the steam methane reactor and flow junctions contain stationary mass and energy balances and pressure losses are assumed to be constant. The molar steam to carbon ratio before the pre-reformer is assumed to be constant at 5.109.

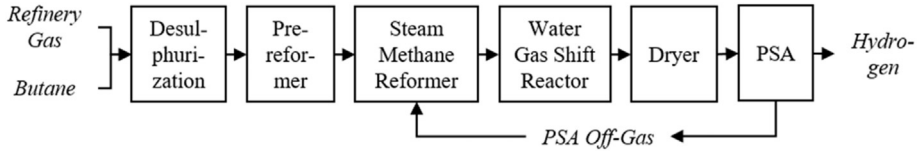

Fig. 3 – Main components and material flows of the refinery system.

Table 1 – Simulation input parameters ([1]calculated from measured data).

Refinery System		
Bed porosity [51]	0.5734	–
Catalyst porosity [39]	0.5196	–
Catalyst specific heat capacity [52]	949.7	J/kgK
Flame area [39]	0.01	m^2
Emissivity of the flue gas [39]	0.1	–
Emissivity of the flames [39]	0.1	–
Emissivity of the tubes [39]	0.95	–
Adiabatic flame temperature [39]	2200	K
Molar steam to carbon ratio at entry of prereformer[1]	5.109	–
Effectiveness factors for the three reactions[1]	0.008504	–
	0.000995	–
	0.005069	–
Refinery gas, butane, natural gas, water, air inlet, ambient, and ground temperature [53]	9.33	°C
Water and air inlet pressure [53]	1.013	bar
Average CO conversion in WGS1	98.93	%
Average PSA efficiency[1]	82.36	%
Constant hydrogen pressure at consumer [33]	30	bar
Trailer		
Minimum trailer pressure [54]	20	bar
Maximum trailer pressure [54]	525	bar
Geometric trailer volume [54]	30.884	m^3
Trailer heat transfer area [54]	427.9	m^2
Inner heat transfer coefficient of trailer [55]	60	W/m^2K
Outer heat transfer coefficient of trailer [55]	6	W/m^2K
De-/Coupling time [54]	15	min
Filling/Discharging time [54]	60	min
Driving time [56]	25	min
Driving distance [56]	22.85	km
Specific diesel consumption [57]	0.35	l/km
Storages		
Specific heat capacity of steel [50]	490	J/kgK
Thermal conductivity of steel [50]	40	W/mK
Density of steel [50]	7800	kg/m^3
Inner heat transfer coefficient of cavern [43]	133	W/m^2K
Inner heat transfer coefficient of other storages [55]	4	W/m^2K
Outer heat transfer coefficient of aboveground storages [55]	3	W/m^2K
Thickness of surrounding salt of cavern that changes temperature [43]	2	m
Constant surrounding salt temperature [43]	44	°C
Height to diameter relation of cavern and high-pressure vessels [43]	6.51	–
Specific heat capacity of salt [58]	840	J/kgK
Thermal conductivity of salt [58]	4	W/mK
Density of salt [58]	3295	kg/m^3
Wall thickness of high pressure vessels, trailers, and cylindrical buffer storages [54]	0.05	m
Diameter of pipe storage [59]	1.4	m
Diameter of cylindrical buffer storage [31]	2.15	m
Wall thickness of pipe storage [59]	0.0255	m
Wall thickness of spherical storage [60]	0.03	m
Gas grid		
Constant pressure at transfer stations of the gas grid [61]	17	bar
Constant gas composition at transfer stations of the gas grid [CH4, C2H6, C3H8, C4H10, N2, CO2] [62]	[72.2, 14.0, 6.9, 1.9, 2.7, 2.3]	wt.-%
Integral roughness of ring pipelines of the NG grid (steel) [46]	0.2	mm
Integral roughness of central pipelines of the NG grid (steel) [46]	0.5	mm

- **Heat exchangers:** The heat exchangers are modeled with a constant outlet temperature or a given heat flow depending on the application.
- **Prereformer:** In the prereformer, the higher hydrocarbons (ethane, propane and butane) are decomposed completely into carbon monoxide and methane by consuming steam. The heat of reaction is considered in the energy balances.
- **SMR:** The model of the steam methane reformer is taken from Ref. [39]. The effectiveness factors for the three occurring reactions and the pressure loss are assumed to be constant and one control volume is used to simplify the model. The effectiveness factors were tuned to fit the measurement data and are listed in the table.
- **WGS reactor:** In the water gas shift reactor, carbon monoxide reacts with steam to carbon dioxide and hydrogen with a constant conversion rate of 98.93% and under consideration of the heat of reaction.
- **Purification:** In the dryer, water is extracted completely from the stream; the pressure swing adsorption has a constant hydrogen recovery rate 82.36%.

- **Burner:** The combustion in the burner is ideal, all components are decomposed completely and their net calorific values are taken into account in the energy balances.

Electrolyzer: The electrolyzer is modeled with an efficiency characteristic curve from measured data published by Refs. [40,41] of an existing 3.75 MW_{el} PEM electrolyzer system in Mainz, Germany. The minimal system power is at 4% of the nominal power and it can be operated at 168% overload for 30 min with the same cooldown time at nominal power or below [42]. A nominal efficiency of 75% related to the gross calorific value of hydrogen is assumed. The output pressure and temperature are 35 bar and 9.33 °C, respectively. Since the start-up time is only about 10 s, an instantaneous response to a power change is assumed.

Hydrogen Storage: Hydrogen storages are modeled with one finite gas volume, the geometric volume, and with variable pressures and temperatures which are defined by instationary mass and energy balances where the heat transfer with the surrounding medium is considered. The heat transfer area is calculated according to the geometric setup of the regarded storage. For salt caverns the surrounding material and heat transfer is considered as done by Ref. [43].

Compressors and Pumps: The pump model is based on a model of the *ClaRa Library* [44,45]. All compressor and pump models have constant mechanical and electrical efficiencies of 96% and 95%, respectively [46]. The ionic compressors are assumed to be isothermal and the compressors used in the refinery are modeled with a constant isentropic efficiency of 80% [46].

Pipelines: The pipeline models are based on a finite volume model of the *ClaRa Library*. In the approach, an adjustable number of finite volumes with one-dimensional instationary mass and energy balances is considered. For the simulation of hydrogen admixture and thus dynamically changing composition and gas properties, the models are augmented for instationary component mass balance calculations. For the high pressure natural gas and hydrogen pipelines, quadratic pressure losses are considered. Especially for the H2NG scenario and admixture of hydrogen the change in density must be considered.

Trailers: For the trailers, a pressure vessel model is used and the in- and outcoming mass flows are controlled depending on the pressure and time to ensure that the trailer pressure is kept within its boundaries as well as the coupling, decoupling, filling, discharging and driving times. The diesel consumption is calculated with a constant specific fuel consumption over the driving distance and for the emissions, specific CO_2 emissions of 266 g/kWh are used [47].

Fluid properties: The thermodynamic states and fluid properties are calculated by Soave-Redlich-Kwong equation of state (EOS) [48] for hydrogen and by Peng-Robinson EOS [49] for natural gas and refinery gas mixtures. Within the steam reformer ideal gas is assumed. The interface for the property calculations is provided by the *TILMedia Suite* [50] and used fluids and fluid mixtures are freely available within the *ClaRa Library*.

Simulation

General: The location of the PtGP (see Fig. 1) was chosen for multiple reasons. A connection to the high voltage grid is available and underground salt domes can be exploited for storage. The site is also preferable for the H2NG scenario because hydrogen is admixed directly after the gas transfer station (GTS) *Reitbrook*, from where about 41% of the consumed natural gas is imported. Thus, more hydrogen can be injected by at the same time keeping the gas quality standards. According to [63,64], under 10 vol.-% of hydrogen admixture are usually possible which is assumed as a maximum for the H2NG scenario. Gas consumers are assumed to control their gas demand according to the gross calorific value, so that imported natural gas masses decrease by the local hydrogen admixture. At the GTS, gas temperature and pressure as well as composition are assumed constant. For H2NG, the high-pressure gas grid of Hamburg, which consists of a ring and a central grid, is modeled in a simplified way. Hamburg is divided into its seven districts and to each district one off-take point from the ring grid is assigned. For the ring grid, parallel pipelines between those points are bundled with equivalent diameters and lengths. For each district, the containing central gas grid is replaced by one equivalent pipeline with one equivalent consumer at its end. The total gas demand is divided to the seven district consumers according to their respective heat demand shares calculated by the gas standard load profile procedure [65] by aggregating building utilization types with data from Ref. [66] for each district.

Replaceable hydrogen in the refinery: The substitution of hydrogen, which is produced by steam reforming, is limited by several parameters. First, the refinery gas has to be consumed and a minimum butane mass flow is necessary to be able to change the load of the steam reformer in short time. Second, the steam reformer has a minimal load which cannot be underrun. Thus, the hydrogen, which is produced in the SMR using butane, can only be substituted within these limits. The average hydrogen production from butane is calculated using a linear least-squares problem including the measurements from gas chromatography and the boundary condition that an increase in hydrocarbons must always lead to an increase in hydrogen production. The substitutable hydrogen production is determined using data from Ref. [33]. In total, 1064.26 tons of hydrogen can be replaced per year, i.e. 8.08% of the total generated hydrogen in the refinery. The hydrogen demand is twice scaled up and down, each - except for the largest scenario - with a scaling factor of three to achieve a higher informative value of the results for different sizes of refineries. The different sizes are referred to as XS (extra small), S (small), M (medium = reference), L (large) and XL (extra large) in the following. For XL the hydrogen production limit is given by the feed-in limit of hydrogen in the natural gas grid, which leads to a maximum production of 6323.16 tons.

The steam to carbon ratio in front of the prereformer as well as the CO conversion rate and the hydrogen recovery rate of the PSA are calculated from the measured data and averaged over the whole year. The effectiveness factors are determined by fitting the model's hydrogen output with the measured data. The simulated refinery gas mass flow is

slightly smaller (0.7%) due to measurement errors and deviations of the model compared to reality.

Electrical residual load and natural gas flow: The scenarios RE+ and RE++ are constructed using projections based on the current German climate policies for the years 2035 and 2050 [2]. If the targets are tightened, the scenarios will be still valid but they will correspond to years before 2035 and 2050, respectively. For RE+ the installed capacities of conventional and renewable power generators are taken from Ref. [67] for the year 2035 and linearly scaled to Hamburg by the respective gross electricity consumptions of Germany (629.8 TWh_{el} [68]) and Hamburg (12.9 TWh_{el} [69]) in 2012. For RE++, it is assumed that the conventional capacities stay the same. The renewable capacities are extrapolated by 15 years according to [70]. Table 2 shows the respective RE capacities. Local combined heat and power (CHP) plants are scheduled according to the heat demand. Furthermore, primary and secondary power reserves according to [71] are considered. Power curves are taken from measured data of [72–75] for wind and solar plants and normalized by installed capacities from Ref. [76] and from Ref. [77] for run-of-river power plants. The unit commitment schedule for the dispatchable power plants was cost-optimized via mixed integer linear programming as stated in Ref. [78]. The resulting negative residual load, which is the difference of electric power demand and non-dispatchable power plants (variable renewables, CHP and must-run reserve power), is shown in Fig. 4 together with the gas demand [61,79], maximum hydrogen admixture at the PtG site, and replaceable hydrogen at the refinery for XS, M, and XL sizes. The negative residual loads are highly fluctuating and only allow electrolyzer operating hours of 1432 for RE+ and 3082 for RE++. Comparing the curves in the right diagram, reveals that, for H2NG and the M size refinery, storage would only be necessary during summer, when maximum hydrogen input rates are reached. However, taking the availability of renewable excess power in the left diagram into account changes storage requirements.

Cost and emission calculations: The observed system consists of the PtGP, the transport system and the refinery. For the cost and emission calculation, the differences of the analyzed pathways to the reference system are calculated. The annuity for a period of 20 years, an interest rate of 7%, and no consideration of price change is calculated according to [80] and divided by the produced hydrogen mass (m_{H_2}) to calculate the levelized hydrogen production costs (LCOH).

$$\begin{aligned}\mathrm{LCOH} = \frac{1}{m_{H_2}} \cdot \big(&\Delta C_{\mathrm{capital}} + \Delta C_{\mathrm{O\&M}} + \Delta C_{\mathrm{el.}} + \Delta m_{\mathrm{water}} \cdot c_{\mathrm{water}} \\ &+ \Delta m_{\mathrm{butane}} \cdot c_{\mathrm{butane}} + \Delta m_{\mathrm{diesel}} \cdot c_{\mathrm{diesel}} \\ &+ \Delta m_{\mathrm{NG,refinery}} \cdot c_{\mathrm{NG,large\ consumer}} + \Delta m_{\mathrm{NG,import}} \cdot c_{\mathrm{NG,import}} \\ &+ \Delta m_{CO_2} \cdot c_{CO_2-\mathrm{certificate}}\big)\end{aligned} \quad (1)$$

LCOH is calculated from a macroeconomic view, including also CO_2 emission reductions and related costs. Considered capital and O&M related costs are displayed in Table 3. Since only differences are calculated, capital and O&M costs of the natural gas grid and the refinery do not influence the results. Relevant energy in- and outputs are shown in Fig. 2. For the refinery, water and electricity consumption of the compressors and the inputs and outputs of butane, natural gas, and hydrogen change. With replacement of hydrogen in the refinery, surplus butane is sold (price, s. Table 2) and does not contribute to emissions anymore. In H2NG, substitutable butane is replaced by natural gas. The difference in cost (large consumer NG price, s. Table 2) and emissions compared to butane are calculated. Because of the assumption that within the city the same gas energy (gross calorific value) is consumed, natural gas is displaced by hydrogen. Thus, in M 41.92 GWh less natural gas is imported which can be energetically translated into CO_2 emission and cost (import NG price, s. Table 2) reductions. Cost of production of hydrogen, that is stored at the beginning of the simulated year, is calculated considering the nominal electrolyzer efficiency and the cost for electricity, water, and CO_2 certificates. This gas cannot be used within this year, so it must be considered in the capital-related expenses.

Table 2 – Scenario specific parameters for RE+ and RE++.

	Unit	RE+	RE++
RE capacities			
Biomass plants	MW_{el}	196	227
Run-off water plants	MW_{el}	86	86
Photovoltaic plants	MW_{el}	1225	1378
Wind onshore plants	MW_{el}	1816	2582
Wind offshore plants	MW_{el}	378	639
Prices			
Electricity price (assumption)	€/MWh_{el}	30.0	30.0
Water price [81]	€/m^3	0.00173	0.00173
Diesel price (2011 value [82] projected with [83])	€/l	1.4588	1.6015
Natural gas price (large consumer) [83]	€/MWh	51.5	58.0
Natural gas price (import) [83]	€/MWh	32.0	33.0
Butane price	€/l	0.4664	0.5120
(2018 value [84] projected with [83])	€/kg	0.7812	0.8576
CO_2 certificate price [83]	€/t_{CO2}	52.5	76.0

Design of the components

Electrolyzer, compressor and storage systems are designed to minimize total costs. The dimensioning must be done iteratively in Modelica since operational and dynamic effects influence the results. As the capital cost of the electrolyzer has usually the biggest share, its design is the first step and is the same for all paths but different for the considered refinery sizes and installed RE capacities. It is sized for producing the requested amount of hydrogen under given technical constraints and with the given negative residual power of the respective RE scenario. The electrolyzer is only running when surplus power is available and hence with zero emissions. Hydrogen compressors are designed for the annually occurring peak demand and not necessarily running when surplus renewable power is available. Thus, the average specific CO_2 factors for the simulated electricity mix of Hamburg are considered (RE+: 208.8 g/kWh_{el}, RE++: 151.6 g/kWh_{el}). This also applies for the start gas generation of the storage units.

The design procedure of the storage systems depends on the scenario: For H2NG, H2Pipe and H2Trailer the main storages after the electrolyzer are designed so that the defined

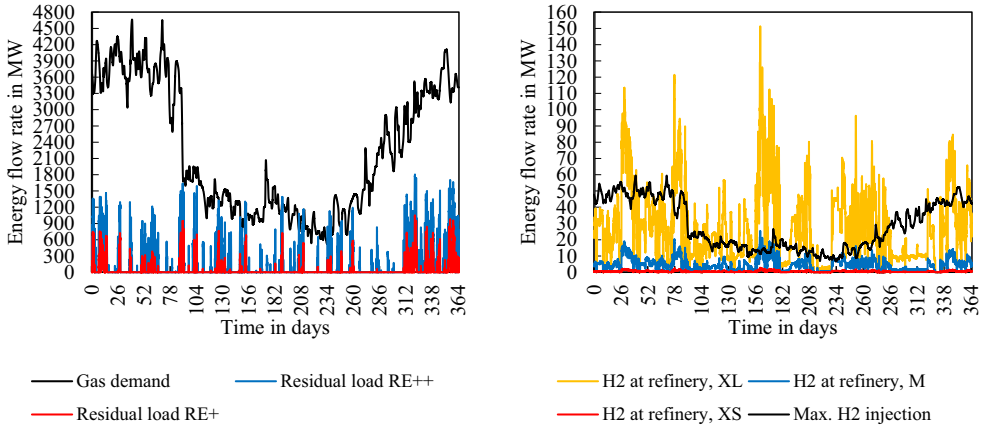

a) Gas demand and electrical residual loads of Hamburg.

b) Replaceable hydrogen at the refinery for XS, M, and XL, and maximum hydrogen injection into the natural gas grid.

Fig. 4 – Annual courses of important input variables.

Table 3 – Capital and O&M related costs of the electrolyzer, compressor, storage, and transport systems.

Component	Capital cost	Yearly O&M cost in % of capital cost	Lifetime
Electrolyzer (35 bar)	RE+: 576 €/kW_{el} · $P_{el,n}$ [12] RE++: 450 €/kW_{el} · $P_{el,n}$ [12]	4% [31]	30 a [31]
Ionic compressor	2083 €/kW_{el} · $P_{el,n}$ [31]	6% [31]	30 a [31]
Salt cavern (58 … 175 bar)	15 · 10^6 € + 19.33 €/m^3 · V_{geo} [57]	2% [31]	30 a [31]
Buried pipe storage (<100 bar)	12 · 10^6/6800 €/m^3 · V_{geo} [85]	2% [31]	50 a [85]
Cylindrical buffer storage (80 bar)	300000/82 €/m^3 · V_{geo} [31]	2% [31]	30 a [31]
Spherical storage vessel (20 bar)	162.37 € · (V_{stp}/m^3)$^{0.8658}$ [60]	2% [31]	30 a [31]
Pipeline	(133.3 €/m + 916.7 €/m^2 · D) · L [86]	2% [86]	30 a [57]
Truck	160000 € [57]	13.05% [57]	12 a [57]
Trailer	700000 € [54]	1.7% [57]	20 a [57]
Filling station	250000 € [31]	3% [31]	30 a [31]

maximum pressure is never reached but closely. For H2Pipe and H2Trailer, the same applies for the minimum pressure and for H2Trailer for the buffer storage as well. For the latter, cavern storages were not considered to ensure independence of geological conditions at the consumer site. The pressures and temperatures in the storages at the end of the simulated year must be the same as in the beginning of the year to ensure periodic operation. By cost-optimization, the least expensive storage type for each scenario is chosen, without neglecting the feasibility of the geometric volumes and the cost for compression however.

In H2NG, for the pressure drop calculation in the model, a nominal point (pressure loss and mass flow rate) must be determined for each pipe segment of the gas grid and for a nominal gas composition and temperature. This is done iteratively for a compressible and isothermal flow and with the annual mean gas demand flow rate at the consumer site.

In H2Pipe, the pipeline layout was assumed to be next to the existing high pressure natural gas pipeline, resulting in a length of 39.15 km. The demanded hydrogen is always fed into the pipeline directly and withdrawn at the refinery site. The pipeline is designed to have minimal size but to be able to work as a buffer storage for fast load changes as well. Furthermore, the pressure losses should be small so that the pipeline pressure is always between electrolyzer and consumer pressure allowing a maximum pressure drop of 5 bar. The nominal pressure loss is calculated using the average hydrogen demand and a surface roughness of 0.04 mm [46]. The resulting diameters are 0.06 m (XS), 0.09 m (S), 0.13 m (M), 0.19 m (L) and 0.25 m (XL).

For H2Trailer, the number of trailers is chosen by cost-optimization in combination with the buffer storage and corresponding compressors. Considering an availability of the trailers of 4380 h per year, only two trailers are needed to meet the demand of the scenarios XS and S. For M, L and XL, 4, 8 and 16 trailers are necessary respectively. The trailer properties are taken from Ref. [54] (NT2).

Results

Technical results

Important results of all scenarios are summarized in Table 4. It shows the replaced amount of hydrogen, which is normally produced by the SMR in the refinery for sizes XS to XL. For the two scenarios of installed RE capacities, the five refinery scales, and the three transportation pathways, average efficiencies of the electrolyzer and the overall system, optimum storage types and their geometric volumes, diameters of the hydrogen pipeline, number of trailers, levelized CO_2 emission and levelized cost differences compared to the reference

system, CO_2 abatement costs, and important sensitivities are summarized. Comparing the dimensions of the components of the PtGP reveals that they are smaller for RE++ compared to RE+. The reason for this is the higher availability of surplus renewable power, so that a smaller PtGP can generate the same hydrogen amount. The efficiencies are calculated using all energy flows, i.e. electric energy for the electrolyzer and compressors, diesel for the trailers, inflowing feed to the SMR and outflowing hydrogen. The reference case, i.e. the steam reformer system, has an efficiency of 80.76%. H2Pipe and H2Trailer lead to an increase in overall efficiency compared to the reference case which is caused by the higher part load efficiency of the refinery system. H2NG is the least efficient because there are two energy conversions in series (PtGP and SMR), whereas in the other scenarios the two conversions are in parallel. H2Pipe is slightly more efficient than H2Trailer, which is caused by the extra diesel consumption and additional electric energy for compression of the latter. In most cases, a salt cavern is the most feasible storage option. For H2NG RE + XS and RE++ XS and S no storage is necessary, because the small generated hydrogen mass flow can at all times be injected into the natural gas grid without exceeding the limit. For RE + S an aboveground cylinder and for the M sizes buried pipe storages are most cost-efficient. Pipe storages are also used for the XS sizes of H2Pipe and H2Trailer. For bigger amounts of hydrogen cavern storages are always the best option. The second storage at the refinery site in H2Trailer is in most cases a spherical container. Only for the L sizes for both RE scenarios pipe storages are more cost-efficient. Spherical storages are usually cheaper for medium and pipe storages for bigger hydrogen amounts. As the number of trailers can only take whole numbers, the optimum point shows a smaller trailer to hydrogen relation for L than for the other scales, so that a bigger storage volume is necessary.

CO_2 emissions and costs

The resulting levelized CO_2 emission reductions compared to the reference refinery system are displayed in Table 4. In most cases, comparing each path and size, CO_2 emission reductions are slightly higher for RE++ due to less electricity consumption of compressors and for start gas generation as well as the lower specific CO_2 emissions of the electricity mix. Although, the chemical substitution of hydrogen in the SMR for H2Pipe and H2Trailer is more efficient than the energetic replacement of natural gas for H2NG, the CO_2 reduction is bigger for the latter, which is due to two effects. First, since the natural gas grid functions as part of the storage, less storage volume and compressor power are needed, which leads to less electricity consumption. The second reason is the displacement of natural gas by hydrogen in the natural gas infrastructure of Hamburg. H2Pipe has a higher impact on CO_2 emission reduction than H2Trailer because no diesel and less electricity is consumed due to smaller storage volumes and compressor powers. On average the levelized CO_2 reductions are 8.20 t_{CO2}/t_{H2} for H2NG, followed by H2Pipe with 8.12 t_{CO2}/t_{H2} and at last H2Trailer with 7.97 t_{CO2}/t_{H2}.

The levelized hydrogen production costs are shown in Fig. 5. Due to smaller dimensions of all components and the smaller electrolyzer size and investment cost, costs are lower for RE++ than for RE+. In H2NG, costs increase with increasing hydrogen amounts, which is mainly caused by the bigger electrolyzer dimensions. Only for RE++ H2NG XL the costs decrease due to strongly decreasing specific storage cost. For H2Pipe and RE+ and H2Trailer for both RE scenarios, the diagram reveals an optimum cost point for the L size. For lower amounts of hydrogen, costs are higher due to higher levelized transport and storage costs. This is especially visible for the XS scenarios where the transport costs by pipeline and trailer, respectively, are very high. Fig. 6, in which main cost contributors are displayed for XS, M, and XL, shows this effect. Pipeline and trailer costs are summarized under other capital costs together with compressor costs. After the optimal cost point, the higher electrolyzer investment expenses cannot be compensated by lower transport and storage costs anymore because the electrolyzer has to be disproportionally big due to the limited amount of excess power.

Fig. 6 shows the main cost factors on the hydrogen production cost. As they are calculated as differences compared to the reference system, negative values indicate a reduction. This is the case for CO_2 costs and other demand-related costs due to less SMR operation. Electrolyzer capital cost is equal for all pathways for the respective RE scenario and hydrogen amount since electrolyzer sizes are the same. For RE+, levelized electrolyzer capex increases significantly with refinery size, which is due to the very limited renewable surplus energy. For RE++, on the other hand, this effect is very small caused by higher excess power availability. With an assumed electricity price of 30 €/MWh_{el}, demand-related electricity costs have a medium impact in most cases and an even higher share on total expenses for RE++ caused by lower electrolyzer investments compared to RE+. In H2NG, storage costs have very little impact, which is the main reason for its cost-efficiency. For XS, S, and M it is the most competitive pathway. For L and XL, costs in H2Pipe are lower than in H2NG. This can be explained by the decrease in the other demands which is higher for H2Pipe and H2Trailer than for H2NG. Other demands include water for the electrolyzer, the difference in water and butane demand for the SMR, and for H2NG the difference in natural gas demand. The latter two result in revenues which are lower for H2NG because butane is partly replaced by the higher-priced natural gas. For all cases, H2Trailer is the most expensive pathway. In other studies, the finding was that trailers are usually more cost-efficient for smaller amounts of hydrogen. The difference in this work is that only one consumer and a small distance between PtGP and refinery is considered. The more consumers with low demand at different locations must be supplied and the longer the distance, the more competitive is the transportation via trailers.

The relative influence in a change of the electricity price is shown in Fig. 7 (left) and the absolute sensitivity in Table 4. In general, scenarios for RE++ are slightly more sensitive than for RE+ with averaged values across all scenarios of 0.05652 (€/kg)/(€/MWh_{el}) and 0.05641 (€/kg)/(€/MWh_{el}), respectively. The reason is that the average electrolyzer efficiency is higher for RE + than for RE++. The lower availability of excess power for RE + leads to bigger electrolyzer dimensions and a higher operation time in part load with higher efficiencies. Thus, the

Table 4 – Resulting dimensions of the components and results of the simulations and sensitivity analysis (compr.: compressor, eff.: efficiency, ely: electrolyzer, LCOH: levelized cost of hydrogen, sens.: sensitivity).

			RE+					RE++				
			XS	S	M	L	XL	XS	S	M	L	XL
All	Replaceable hydrogen	t	118.25	354.75	1064.26	3192.78	6323.16	118.25	354.75	1064.26	3192.78	6323.16
	Nominal ely power	MW_{el}	3.4	10.7	34.0	118.5	352.8	1.6	4.8	14.6	45.3	93.4
	Average ely eff.	%	71.30	71.41	71.59	72.29	74.79	71.22	71.23	71.29	71.39	71.58
H2NG	Storage type		none	80 bar cylinder	100 bar pipe	cavern	cavern	none	none	80 bar pipe	cavern	cavern
	Main geometric storage volume	m^3	0	82	2600	42000	285000	0	0	1380	12425	164300
	Nominal compr. power	kW_{el}	0	32.9	245.8	1391.6	5454.3	0	0	56.9	604.2	1116.3
	Overall system eff.	%	73.81	73.82	73.83	73.87	74.06	73.80	73.80	73.81	73.80	73.80
	Levelized CO_2 reduction	t_{CO2}/t_{H2}	−8.218	−8.218	−8.216	−8.175	−8.147	−8.222	−8.222	−8.222	−8.207	−8.185
	LCOH	€/kg	2.00	2.19	2.70	3.25	4.55	0.46	0.47	0.73	1.08	0.94
	CO_2 abatement cost	$€/t_{CO2}$	244	266	329	397	558	56	57	88	131	115
	Sens. towards electricity cost	$(€/kg)/(€/MWh_{el})$	0.05532	0.05524	0.05512	0.05521	0.05469	0.05538	0.05537	0.05534	0.05543	0.05634
	Sens. towards ely capital cost	$(€/kg)/(€/kW_{el})$	0.00367	0.00379	0.00403	0.00469	0.00704	0.00168	0.00170	0.00173	0.00179	0.00187
	Sens. towards CO_2 certificate cost	$(€/kg)/(€/t_{CO2})$	−0.00822	−0.00822	−0.00821	−0.00808	−0.00781	−0.00822	−0.00822	−0.00822	−0.00819	−0.00803
H2Pipe	Storage type		100 bar pipe	cavern	cavern	cavern	cavern	100 bar pipe	cavern	cavern	cavern	cavern
	Main geometric storage volume	m^3	5930	18700	57600	181000	374000	3740	11700	35700	111000	229000
	Pipeline diameter	m	0.06	0.09	0.13	0.19	0.25	0.06	0.09	0.13	0.19	0.25
	Nominal compr. power (sum)	kW_{el}	47.9	176.4	561.6	1972.0	5934.0	35.8	79.59	242.9	752.3	1551.0
	Overall system eff.	%	81.08	81.07	81.09	81.16	81.39	81.08	81.07	81.07	81.08	81.10
	Levelized CO_2 reduction	t_{CO2}/t_{H2}	−8.135	−8.096	−8.096	−8.096	−8.095	−8.145	−8.124	−8.124	−8.124	−8.123
	LCOH	€/kg	16.88	8.70	4.31	3.12	4.01	11.81	6.73	2.21	0.66	0.29
	CO_2 abatement cost	$€/t_{CO2}$	2074	1075	532	386	496	1451	829	272	81	35
	Sens. towards electricity cost	$(€/kg)/(€/MWh_{el})$	0.05638	0.05761	0.05751	0.05704	0.05535	0.05606	0.05688	0.05686	0.05683	0.05675
	Sens. towards ely capital cost	$(€/kg)/(€/kW_{el})$	0.00367	0.00379	0.00403	0.00469	0.00704	0.00168	0.00170	0.00173	0.00179	0.00187
	Sens. towards CO_2 certificate cost	$(€/kg)/(€/t_{CO2})$	−0.00791	−0.00764	−0.00763	−0.00761	−0.00759	−0.00803	−0.00791	−0.00790	−0.00790	−0.00789
H2Trailer	Main storage type		100 bar pipe	cavern	cavern	cavern	cavern	100 bar pipe	cavern	cavern	cavern	cavern
	Main geometric storage volume	m^3	6000	18700	57600	181000	375000	3800	11700	35600	111000	228000
	Buffer storage type		spherical	spherical	spherical	100 bar pipe	spherical	spherical	spherical	spherical	100 bar pipe	spherical
	Geometric buffer storage volume	m^3	107	325	492	3920	35100	111	331	492	3920	35100
	Number of trailers		2	2	4	8	16	2	2	4	8	16
	Nominal compr. power (sum)	kW_{el}	2137.2	1234.9	1935.9	4083.9	15168.0	2098.9	1131.67	1533.2	2816.3	11015.0
	Overall system eff.	%	80.93	80.99	81.01	81.09	81.31	80.96	80.97	81.04	81.00	81.00
	Levelized CO_2 reduction	t_{CO2}/t_{H2}	−7.943	−7.936	−7.940	−7.959	−7.932	−7.985	−7.981	−7.984	−7.998	−7.980
	LCOH	€/kg	21.22	8.99	4.99	3.98	5.46	16.08	7.03	2.87	1.51	1.64
	CO_2 abatement cost	$€/t_{CO2}$	2671	1133	629	500	689	2014	880	360	189	206
	Sens. towards electricity cost	$(€/kg)/(€/MWh_{el})$	0.05708	0.05814	0.05802	0.05752	0.05595	0.05682	0.05753	0.05747	0.05739	0.05742
	Sens. towards ely capital cost	$(€/kg)/(€/kW_{el})$	0.00367	0.00379	0.00403	0.00469	0.00704	0.00168	0.00170	0.00173	0.00179	0.00187
	Sens. towards CO_2 certificate cost	$(€/kg)/(€/t_{CO2})$	−0.00772	−0.00748	−0.00747	−0.00747	−0.00742	−0.00787	−0.00776	−0.00777	−0.00777	−0.00774

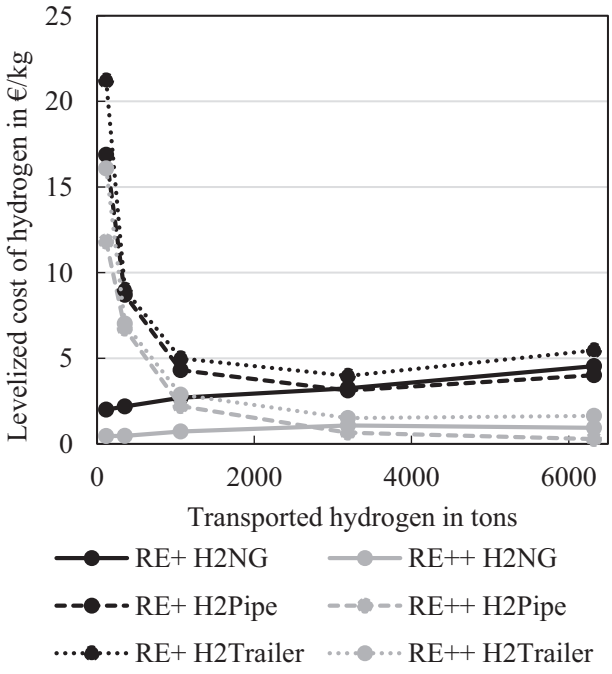

Fig. 5 – Levelized cost of hydrogen over transported hydrogen amounts (the dots mark the sizes XS-XL).

lower electricity consumption of the electrolyzer compensates the higher consumption for cushion gas generation. In tendency, the sensitivities decrease with increasing electrolyzer size within each RE scenario except for the XS scenarios that have a small sensitivity due to low demand for compression. The figure reveals that RE++ H2Pipe XL is most sensitive to a change in electricity price. A decrease of approximately 16.8% in electricity price would be sufficient for 100% reduction and thus zero LCOH. On the other hand, an equivalent increase would double LCOH for this scenario. The shown RE++ H2NG scenarios are also very sensitive and can reach zero LCOH with reductions of 27.6% (XS) up to 55.6% (XL). For RE++ H2Trailer XL, reductions of approximately 95.2% are necessary for zero LCOH. All other shown scenarios require negative electricity prices.

In Europe, CO_2 is traded at the European Stock Exchange (EEX) [87]. In 2016, the average price was very low with 5.12 €/t_{CO2} [88] but an increase is predicted [83] and can already be observed for the last year's development. Fig. 7 (right) shows how much the CO_2 price would have to increase to achieve zero hydrogen production cost. The differences between the configurations are significant. With a CO_2 price of 93 €/t_{CO2}, RE++ H2Pipe XL would deliver hydrogen for no cost whereas for RE + H2Trailer XS 2778 €/t_{CO2} would be necessary. Table 4 also reveals the CO_2 abatement cost, i.e. the cost to reduce one ton of CO_2, for each scenario. They are lower for RE++ and show the same behavior as the levelized cost of hydrogen in Fig. 5. On average they are also lower for the H2NG pathways and always highest for H2Trailer looking at the respective RE scenario and size. H2Pipe gets more cost-competitive for bigger sizes. For both RE scenarios and L and XL sizes, CO_2 abatement costs are lowest for this pathway.

Another impact factor is the capital cost of the electrolyzer that influences the O&M cost as well, see Fig. 8. Starting with 576 €/kW_{el} for RE+ and 450 €/kW_{el} for RE++, cutting capital cost in half signifies an average decrease in levelized cost of hydrogen of 1.34 €/kg (21.9%) for RE+ and of 0.39 €/kg (26.7%) for RE++. The sensitivity increases with increasing electrolyzer sizes. For H2Pipe and H2Trailer in the RE + scenario for XS and S, storage cost has an even higher impact on total cost than the electrolyzer. In the RE++ scenario this is even the case for most of the refinery scales (H2Pipe XS-M, H2Trailer XS-L).

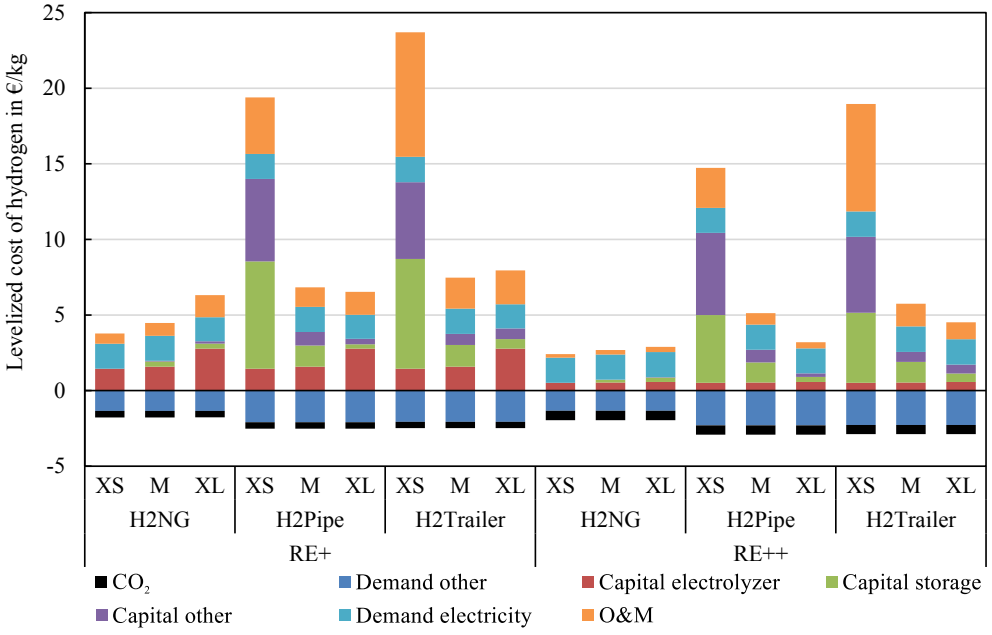

Fig. 6 – Levelized cost of hydrogen of main cost factors for all pathways, XS, M, and XL refinery scales and both RE scenarios. Subtracting negative from positive portions results in hydrogen production cost.

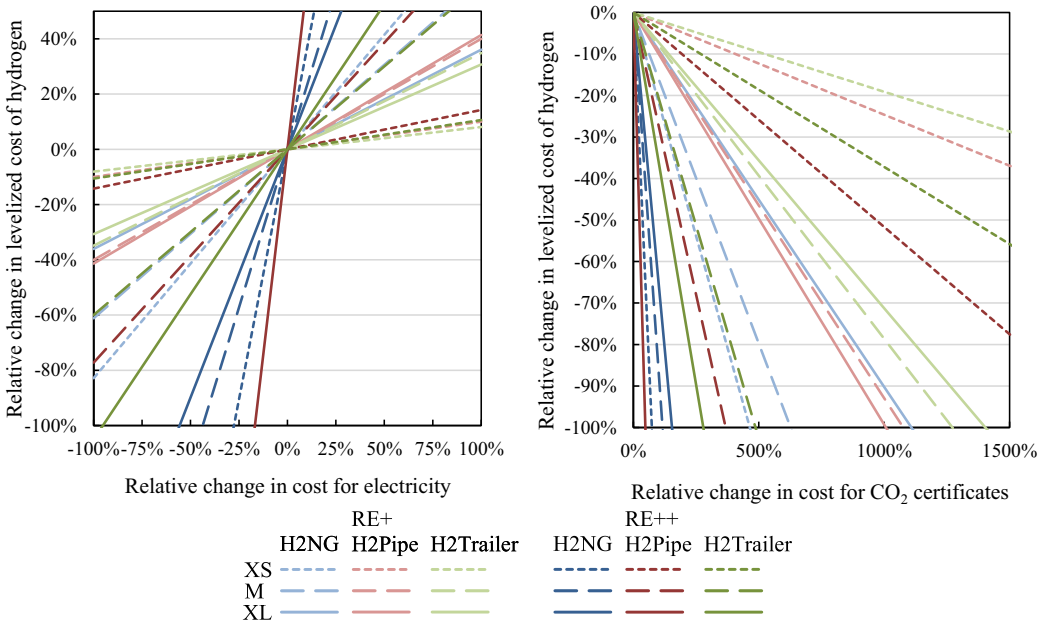

Fig. 7 – Sensitivity analysis for electricity price (left, 0% equals 30 €/MWh$_{el}$) and CO_2 certificate price (right, 0% equals 52.5 €/t$_{CO2}$ (RE+) and 76 €/t $_{CO2}$ (RE++)) on hydrogen production cost.

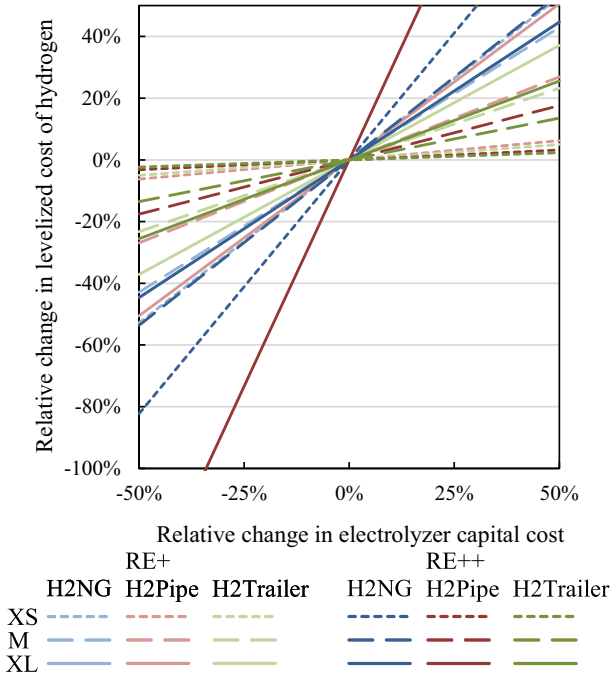

Fig. 8 – Sensitivity analysis for electrolyzer capital cost (0% equals 576 €/kW$_{el}$ (RE+) and 450 €/kW$_{el}$ (RE++)) on hydrogen production cost.

Conclusions

The analysis of the refinery revealed a substitution potential of 8.08% (1064.26 tons) of the annual hydrogen demand that could be produced by a PtGP. In a variation this amount was scaled up and down twice and transported by either the natural gas grid, a hydrogen pipeline or by trailers. Furthermore, two scenarios with installed renewable energy capacities and resulting excess power were considered. Depending on the transported amount of hydrogen, different storage sizes and thus different technologies are most cost-competitive. For H2NG storage volumes are smallest and for little hydrogen amounts not necessary since the natural gas grid functions as storage up to a hydrogen feed-in limit of 10 vol.-%. Except for the XS sizes, where pipe storages are used, salt caverns are the best storage option for H2Pipe and H2Trailer. For the latter pathway, an additional buffer storage - mostly a spherical storage - at the consumer site reduces costs further.

All scenarios showed a CO_2 reduction and thus can help meeting the climate goals until the more effective Power-to-Liquid processes are economically feasible. Each of the RE++ scenarios always lead to lower cost and higher CO_2 reductions than its corresponding RE + scenario. The lower cost result from higher full load hours of the electrolyzer. A stronger increase in full load hours might lead to even lower cost but the electricity price would rise as well then.

H2Pipe and H2Trailer both lead to a slight increase in the overall efficiency compared to the reference system. It is highest for H2Pipe and lowest for H2NG with on average 81.12% and 73.84%, respectively. On the other hand, CO_2 reductions are highest for H2NG with on average 8.20 t_{CO2}/t_{H2}, followed by H2Pipe with 8.12 t_{CO2}/t_{H2} and at last H2Trailer with 7.97 t_{CO2}/t_{H2}. The cost analysis showed that H2NG is most cost-efficient for smaller transported hydrogen amounts while H2Pipe is the preferred choice for bigger transported volumes. Transporting hydrogen via trailers does not convince for any of the sizes and RE scenarios. Thus, trailers are not feasible for only one consumer and a relatively short transportation distance. The same holds true for the CO_2 abatement cost, in

which H2NG is best at the lowest transported hydrogen amount (RE + XS: 244 €/t_{CO2}, RE++ XS: 56 €/t_{CO2}) whereas H2Pipe (RE + L: 386 €/t_{CO2}, RE++ XL: 35 €/t_{CO2}) and H2Trailer (RE + L: 500 €/t_{CO2}, RE++ L: 189 €/t_{CO2}) are best for higher hydrogen amounts. The sensitivity analysis showed a high sensitivity towards the electricity and CO_2 certificate price. With CO_2 prices of 93 €/t_{CO2} - 2778 €/t_{CO2} zero hydrogen production cost can be reached and with free electricity even negative costs can occur (lowest value −1.42 €/kg (RE++ H2Pipe XL), highest value 19.51 €/kg (RE + H2Trailer XS)).

To summarize, Power-to-Gas can play an important role in future coupled energy systems and costs strongly depend on the amount of hydrogen, the transport mechanism and the economic parameters. Multiple usage of the electrolyzer, e.g. for ancillary services, could increase the competitiveness. Additionally, political incentives, e.g. an increase in CO_2 certificate price and/or electricity price tax exemptions, can help to establish this new technology to achieve significant CO_2 reductions in a cross-sectoral manner.

6. Acknowledgements

This work has been conducted within the scope of the research projects *TransiEnt.EE* (BMWi 03ET4003) and *ResiliEntEE* (BMWi 03ET4048). The authors would like to thank the German Federal Ministry of Economic Affairs and Energy (BMWi) for the financial support. Special thanks go to the Holborn Europa Raffinerie.

REFERENCES

[1] UNFCCC. Paris agreement. 2015.
[2] Bundesministerium für Wirtschaft und Energie. Die Energie der Zukunft - Fünfter Monitoring-Bericht zur Energiewende. 2016. Berlin.
[3] BMWi. Zahlen und Fakten Energiedaten. Berlin: Bundesministerium für Wirtschaft und Energie (BMWi); 2017.
[4] Badwal SPS, Giddey S, Munnings C. Hydrogen production via solid electrolytic routes. Wiley Interdiscip Rev Energy Environ 2013;2:473–87. https://doi.org/10.1002/wene.50.
[5] Schiebahn S, Grube T, Robinius M, Tietze V, Kumar B, Stolten D. Power to gas: technological overview, systems analysis and economic assessment for a case study in Germany. Int J Hydrogen Energy 2015;40:4285–94. https://doi.org/10.1016/j.ijhydene.2015.01.123.
[6] Götz M, Lefebvre J, Mörs F, McDaniel Koch A, Graf F, Bajohr S, et al. Renewable power-to-gas: a technological and economic review. Renew Energy 2016;85:1371–90. https://doi.org/10.1016/j.renene.2015.07.066.
[7] Collet P, Flottes E, Favre A, Raynal L, Pierre H, Capela S, et al. Techno-economic and life cycle assessment of methane production via biogas upgrading and power to gas technology. Appl Energy 2017;192:282–95. https://doi.org/10.1016/j.apenergy.2016.08.181.
[8] Judd R, Pinchbeck D. Hydrogen admixture to the natural gas grid. Compend. Hydrog. Energy. Elsevier Ltd.; 2016. p. 165–92. https://doi.org/10.1016/B978-1-78242-364-5.00008-7.
[9] Rönsch S, Schneider J, Matthischke S, Schlüter M, Götz M, Lefebvre J, et al. Review on methanation - from fundamentals to current projects. Fuel 2016;166:276–96. https://doi.org/10.1016/j.fuel.2015.10.111.
[10] Meylan FD, Piguet FP, Erkman S. Power-to-gas through CO2 methanation: assessment of the carbon balance regarding EU directives. J Energy Storage 2017;11:16–24. https://doi.org/10.1016/j.est.2016.12.005.
[11] Bazzanella AM, Ausfelder F. Low carbon energy and feedstock for the European chemical industry. 2017.
[12] Verkehrswende Agora, Energiewende Agora. Frontier economics. Die zukünftigen Kosten strombasierter synthetischer Brennstoffe. 2018. Berlin.
[13] Schmidt P, Batteiger V, Roth A, Weindorf W, Raksha T. Power-to-Liquids as renewable fuel option for aviation: a review. Chem Ing Tech 2018;90:127–40. https://doi.org/10.1002/cite.201700129.
[14] Walker SB, Van Lanen D, Fowler M, Mukherjee U. Economic analysis with respect to power-to-gas energy storage with consideration of various market mechanisms. Int J Hydrogen Energy 2016;41:7754–65. https://doi.org/10.1016/j.ijhydene.2015.12.214.
[15] Al-Subaie A, Maroufmashat A, Elkamel A, Fowler M. Presenting the implementation of power-to-gas to an oil refinery as a way to reduce carbon intensity of petroleum fuels. Int J Hydrogen Energy 2017;42:19376–88. https://doi.org/10.1016/j.ijhydene.2017.06.067.
[16] McKenna RC, Bchini Q, Weinand JM, Michaelis J, König S, Köppel W, et al. The future role of power-to-gas in the energy transition: regional and local techno-economic analyses in Baden-Württemberg. Appl Energy 2018;212:386–400. https://doi.org/10.1016/j.apenergy.2017.12.017.
[17] Mukherjee U, Elsholkami M, Walker S, Fowler M, Elkamel A, Hajimiragha A. Optimal sizing of an electrolytic hydrogen production system using an existing natural gas infrastructure. Int J Hydrogen Energy 2015;40:9760–72. https://doi.org/10.1016/j.ijhydene.2015.05.102.
[18] Walker SB, Mukherjee U, Fowler M, Elkamel A. Benchmarking and selection of power-to-gas utilizing electrolytic hydrogen as an energy storage alternative. Int J Hydrogen Energy 2016;41:7717–31. https://doi.org/10.1016/j.ijhydene.2015.09.008.
[19] Lyseng B, Niet T, English J, Keller V, Palmer-Wilson K, Robertson B, et al. System-level power-to-gas energy storage for high penetrations of variable renewables. Int J Hydrogen Energy 2017;43:1966–79. https://doi.org/10.1016/j.ijhydene.2017.11.162.
[20] DOE. DOE H2A delivery analysis: hydrogen and fuel cells program. 2017. October 24, 2017, https://www.hydrogen.energy.gov/h2a_delivery.html.
[21] Yang C, Ogden J. Determining the lowest-cost hydrogen delivery mode. Int J Hydrogen Energy 2007;32:268–86. https://doi.org/10.1016/j.ijhydene.2006.05.009.
[22] Cheng J, Graham PW. Modelling hydrogen fuel distribution. In: 18th world IMACS congr MODSIM09 int congr model simul interfacing model simul with math comput sci proc; 2009. p. 211–7.
[23] Garmsiri S, Rosen M, Smith G. Integration of wind energy, hydrogen and natural gas pipeline systems to meet community and transportation energy needs: a parametric study. Sustainability 2014;6:2506–26. https://doi.org/10.3390/su6052506.
[24] Andresen L, Schmitz G. Bewertung von power-to-gas-anlagen mittels dynamischer Systemsimulation. Gwf-Gas + Energ 2016:682–9.
[25] Stromnetz Hamburg GmbH, Hamburg Stadt. Energieportal Hamburg: Hamburg in Zahlen. 2016. April 12, 2017, http://www.energieportal-hamburg.de/distribution/energieportal/.
[26] Uniper Innovation Energy Storage, HanseWerk AG. WindGas Hamburg. 2016. April 10, 2017, http://www.windgas-hamburg.com/projekt/projektdarstellung/.

[27] Hamburg Netz GmbH. Veröffentlichungen gemäß § 40 Abs. 1 GasNZV. 2016. July 22, 2016, https://www.hh-netz.com/cps/rde/xchg/hamburg-netz/hs.xsl/65.htm.
[28] Schleswig-Holstein Netz GmbH. Veröffentlichungen gemäß §40 Abs. 1 GasNZV. 2016.
[29] Vattenfall Europe Wärme AG. Netzplan Vattenfall Wärme Hamburg. 2012.
[30] QGIS Development Team. QGIS Geographic information system: open source geospatial foundation project. 2016. March 12, 2016, http://qgis.osgeo.org.
[31] Stolzenburg K, Hamelmann R, Wietschel M, Genoese F, Michaelis J, Lehmann J, et al. Integration von Wind-Wasserstoff-Systemen in das Energiesystem. 2014.
[32] Leprince P. Petroleum refining V.3: conversion processes. Paris: Editions Technip; 2001.
[33] Holborn Europa Raffinerie. Personal communication. 2017.
[34] Andresen L, Dubucq P, Peniche Garcia R, Ackermann G, Kather A, Schmitz G. Status of the TransiEnt library: transient simulation of coupled energy networks with high share of renewable energy. In: Proc. 11th int. Model. Conf. Versailles, France: Linköping University Electronic Press, Linköpings universitet; 2015. p. 695–705. https://doi.org/10.3384/ecp15118695.
[35] Andresen L, Dubucq P, Garcia RP, Ackermann G, Kather A, Schmitz G. Transientes Verhalten gekoppelter Energienetze mit hohem Anteil Erneuerbarer Energien: Abschlussbericht des Verbundvorhabens. 2017. Hamburg.
[36] TUHH. TransiEnt Library: transient simulation of coupled energy networks. 2017. October 24, 2017, https://www.tuhh.de/transient-ee/.
[37] Modelica Association. Modelica: a unified object-oriented language for systems modeling, language specification version 3.4. 2017. Linköping, Sweden.
[38] Dassault Systemes. Dymola. 2017. December 1, 2017, http://www.3ds.com/products-services/catia/products/dymola.
[39] Nandasana AD, Ray AK, Gupta SK. Dynamic model of an industrial steam reformer and its use for multiobjective optimization. Ind Eng Chem Res 2003;42:4028–42. https://doi.org/10.1021/ie0209576.
[40] Schönberger D. P2G durch Elektrolyse - eine flexible Speicherlösung. Powertage; 2016.
[41] Kopp M, Coleman D, Stiller C, Scheffer K, Aichinger J, Scheppat B. Energiepark Mainz: technical and economic analysis of the worldwide largest power-to-gas plant with PEM electrolysis. Int J Hydrogen Energy 2017;42:13311–20. https://doi.org/10.1016/j.ijhydene.2016.12.145.
[42] Farchmin F. Personal communication. Siemens AG; 2016.
[43] Tietze V, Stolten D. Comparison of hydrogen and methane storage by means of a thermodynamic analysis. Int J Hydrogen Energy 2015;40:11530–7. https://doi.org/10.1016/j.ijhydene.2015.04.154.
[44] XRG Simulation. TLK-thermo, TUHH. ClaRa library: simulation of Clausius-Rankine cycles. 2017. August 8, 2018, http://www.claralib.com/.
[45] Brunnemann J, Gottelt F, Wellner K, Renz A, Tähring A, Röder V, et al. Status of ClaRaCCS: modelling and simulation of coal-fired power plants with CO_2 capture. In: Proc. 9th Int. Model. Conf., München; 2012. p. 609–18. https://doi.org/10.3384/ecp12076609.
[46] Cerbe G. Grundlagen der Gastechnik. seventh ed. München/Wien: Carl Hanser Verlag; 2008.
[47] Forschungsstelle für Energiewirtschaft e.V.. Basisdaten zur Bereitstellung und Umwandlung von Brennstoffen. Basisdaten von Energieträgern. 2009. p. 1–3. August 8, 2018, https://www.ffe.de/die-themen/erzeugung-und-markt/186.
[48] Soave G. Equilibrium constants from a modified Redlich-Kwong equation of state. Chem Eng Sci 1972;27:1197–203.
[49] Peng D-Y, Robinson DB. A new two-constant equation of state. Ind Eng Chem Fundam 1976;15:59–64. https://doi.org/10.1021/i160057a011.
[50] TLK-Thermo. TILMedia Suite: software package for calculating the properties of thermophysical substances. 2017. August 8, 2018, https://www.tlk-thermo.com/index.php/de/tilmedia-suite.
[51] Pushnov AS. Calculation of average bed porosity. Chem Petrol Eng 2006;42:14–7. https://doi.org/10.1007/s10556-006-0045-x.
[52] Pantoleontos G, Kikkinides ES, Georgiadis MC. A heterogeneous dynamic model for the simulation and optimisation of the steam methane reforming reactor. Int J Hydrogen Energy 2012;37:16346–58. https://doi.org/10.1016/j.ijhydene.2012.02.125.
[53] Deutscher Wetterdienst (DWD). WebWerdis weather request and distribution system: Klimadaten Hamburg-Fuhlsbüttel 2012 (average monthly means). 2016.
[54] Zerhusen. Impact of high capacity CGH2-trailers - deliverable 6.2. 2013.
[55] Olmos F, Manousiouthakis VI. Hydrogen car fill-up process modeling and simulation. Int J Hydrogen Energy 2013;38:3401–18. https://doi.org/10.1016/j.ijhydene.2012.12.064.
[56] Google. Route: Allermöher Deich 449, Hamburg - Holborn Europa Raffinerie. 2017. Hamburg, https://www.google.de/maps/. August 8, 2018.
[57] Stiller C, Schmidt P, Michalski J, Wurster R, Albrecht U, Bünger U, et al. Potenziale der Wind-Wasserstoff-Technologie in der Freien und Hansestadt Hamburg und Schleswig-Holstein. 2010.
[58] Kushnir R, Dayan A, Ullmann A. Temperature and pressure variations within compressed air energy storage caverns. Int J Heat Mass Tran 2012;55:5616–30. https://doi.org/10.1016/j.ijheatmasstransfer.2012.05.055.
[59] Bilfinger Vam Anlagentechnik. Erdgasröhrenspeicher Urdorf/CH. 2017. August 8, 2018, http://www.vam.bilfinger.com/referenzen/tiefrohrleitungsbau/referenzen-gasspeicher/#gallery1337.
[60] Tietze V, Luhr S, Stolten D. Bulk storage vessels for compressed and liquid hydrogen. Hydrog Sci Eng Mater Process Syst Technol 2016;2:659–89. https://doi.org/10.1002/9783527674268.ch27.
[61] Brauer T. Power to Gas Projekt "WindGas Reitbrook. EON Hanse AG; 2013.
[62] HanseWerk AG. THB - Technische Hinweise und Bestimmungen (Gas) für das Netzgebiet der HanseWerk AG. der Hamburg Netz GmbH und der Schleswig-Holstein Netz AG; 2015.
[63] DVGW-Arbeitsblatt G 260. Gasbeschaffenheit. Dtsch Verein Des Gas- Und Wasserfaches DVGW. 2013.
[64] DVGW-Arbeitsblatt G 262. Nutzung von Gasen aus regenerativen Quellen in der öffentlichen Gasversorgung. Dtsch Verein Des Gas- Und Wasserfaches DVGW. 2011.
[65] BDEW, VKU, GEODE. Abwicklung von Standardlastprofilen Gas. BDEW/VKU/GEODE-Leitfaden; 2016.
[66] Landesbetrieb Geoinformation und Vermessung (LGV). Amtliches Liegenschaftskatasterinformationssystem (ALKIS). 2016.
[67] 50Hertz, Amprion, TenneT, TransnetBW. Netzentwicklungsplan Strom 2025 - Zweiter Entwurf der Übertragungsnetzbetreiber. 2016. Berlin; Dortmund; Bayreuth; Stuttgart.
[68] Bundesministerium für Wirtschaft und Energie (BMWi). Zahlen und Fakten. 2016. August 8, 2018, http://www.bmwi.de/DE/Themen/Energie/Strommarkt-der-Zukunft/zahlen-fakten.html.
[69] Stromnetz Hamburg. Veröffentlichung nach §17 Abs. 2 Nr. 2 StromNZV. 2012.

[70] Bundesrepublik Deutschland. Gesetz für den Ausbau erneuerbarer Energien (Erneuerbare-Energien-Gesetz - EEG 2014) vom 21. Juli 2014 (BGBl. I S. 1066), das zuletzt durch Artikel 1 des Gesetzes vom 29. Juni 2015 (BGBl. I S. 1010) geändert worden ist. 2014.
[71] European Network of Transmission System Operators for Electricity (ENTSO-E). P1 – policy 1: load-frequency control and performance [C]. In: ENTSO-E, editor. ENTSO-E oper. Handb. ENTSO-E; 2009.
[72] 50Hertz. Netzkennzahlen. 50Hertz Transm GmbH. 2016. August 8, 2018, http://www.50hertz.com/de/kennzahlen.
[73] Amprion. Netzkennzahlen. Amprion GmbH. 2016. August 8, 2018, http://www.amprion.net/netzkennzahlen.
[74] TenneT, Netzkennzahlen. TenneT TSO GmbH. 2016. August 8, 2018, http://www.tennettso.de/site/Transparenz/veroeffentlichungen/netzkennzahlen.
[75] Transnet BW. Netzkennzahlen. TransnetBW GmbH. 2016. August 8, 2018, https://www.transnetbw.de/de/kennzahlen.
[76] Bundesnetzagentur. Zahlen, Daten und Informationen zum EEG. 2016. August 8, 2018, http://www.bundesnetzagentur.de/DE/Sachgebiete/ElektrizitaetundGas/Unternehmen_Institutionen/ErneuerbareEnergien/ZahlenDatenInformationen/zahlenunddaten-node.html.
[77] Ziems C, Meinke S, Nocke J, Weber H, Hassel E. Kraftwerksbetrieb bei Einspeisung von Windparks und Photovoltaikanlagen. 2012. Rostock.
[78] Dubucq P, Ackermann G. Frequency control in coupled energy systems with high penetration of renewable energies. In: 2015 Int. Conf. Clean electr. Power; 2015. p. 326–32. https://doi.org/10.1109/ICCEP.2015.7177643.
[79] Hamburg Netz GmbH. Veröffentlichungen nach §27 Abs. 2 GasNEV. 2012.
[80] VDI 2067 Blatt 1. Wirtschaftlichkeit gebäudetechnischer Anlagen. Verein Dtsch Ingenieure eV; 2012.
[81] Hamburg Wasser. Gebühren, Abgaben und Preise. 2017. August 8, 2018, https://www.hamburgwasser.de/privatkunden/service/gebuehren-abgaben-preise/.
[82] Destatis. Preise - Daten zur Energiepreisentwicklung. 2017.
[83] Prognos, EWI, GWS. Entwicklung der Energiemärkte – Energiereferenzprognose. Basel Köln Osnabrück; 2014.
[84] Brennstoffhandel. Flüssiggas (DIN 51622) (exkl. MwSt.) - PLZ: 21079. 2017. Menge: 6000 l, http://www.brennstoffhandel.de/. August 8, 2018.
[85] Bünger U, Michalski J, Crotogino F, Kruck O. Large-scale underground storage of hydrogen for the grid integration of renewable energy and other applications. In: Ball M, Basile A, Veziroğlu TN, editors. Compend. Hydrog. Energy. Oxford: Woodhead Publishing; 2016. p. 133–63. https://doi.org/10.1016/B978-1-78242-364-5.00007-5.
[86] Altmann M, Gaus S, Landinger H, Stiller C, Wurster R. Wasserstofferzeugung in offshore Windparks: "Killer-Kriterien", grobe Auslegung und Kostenabschätzung. Ottobrunn; 2001.
[87] EEX. European energy exchange (EEX). 2017. August 8, 2018, https://www.eex.com/en/.
[88] European Energy Exchange AG. Emission spot primary market auction report 2016 - annual average means Germany. 2017.